Reaction dynamics, OH energy partitioning, and OH product angular momentum alignment studies: H+H2O→OH+H2 versus H+CO2→OH+CO

ARTICLE *in* CHEMICAL PHYSICS LETTERS · FEBRUARY 1994

Impact Factor: 1.9 · DOI: 10.1016/0009-2614(93)E1462-P

3 AUTHORS, INCLUDING:

Axel Jacobs
Universität Heidelberg
17 PUBLICATIONS **514** CITATIONS

SEE PROFILE

ELSEVIER

4 February 1994

Chemical Physics Letters 218 (1994) 51–59

CHEMICAL PHYSICS LETTERS

Reaction dynamics, OH energy partitioning, and OH product angular momentum alignment studies: $H+H_2O \rightarrow OH+H_2$ versus $H+CO_2 \rightarrow OH+CO$

A. Jacobs, H.-R. Volpp, J. Wolfrum

Physikalisch-Chemisches Institut der Universität Heidelberg, Im Neuenheimer Feld 253, D-69120 Heidelberg, Germany

Received 8 November 1993

Abstract

Using translationally excited H atoms generated by laser photolysis of H_2S at 193 nm, the reaction dynamics of $H+H_2O \rightarrow OH+H_2$ and $H+CO_2 \rightarrow OH+CO$ was investigated at collision energies of 2.2 and 2.3 eV, respectively. Nascent OH rotational and vibrational quantum-state distributions and OH product translational energies were measured by means of the laser photolysis/laser-induced fluorescence pump–probe technique. A markedly non-statistical distribution of the available energy was found: $H+H_2O \rightarrow OH+H_2$: $f_{rot}=0.04\pm0.01$, $f_{vib}<4\times10^{-3}$, $f_{trans}=0.65\pm0.26$; $H+CO_2 \rightarrow OH+CO$: $f_{rot}=0.14\pm0.02$, $f_{vib}=0.11\pm0.04$, $f_{trans}=0.59\pm0.16$. In addition, velocity-aligned H atoms generated via polarized H_2S photodissociation were used to investigate vector correlations for both reactions.

1. Introduction

The reactions

$$H+H_2O \rightarrow OH+H_2, \quad \Delta H^0_{298}=62\ \text{kJ/mol}, \qquad (1)$$

$$H+CO_2 \rightarrow OH+CO, \quad \Delta H^0_{298}=102\ \text{kJ/mol}, \qquad (2)$$

$$H+O_2 \rightarrow OH+O, \quad \Delta H^0_{298}=69.5\ \text{kJ/mol}, \qquad (3)$$

together with the corresponding reverse reactions (−1), (−2), and (−3), have been found to play a central role in a variety of combustion and atmospheric processes [1]. Besides their great practical importance, reactions (1), (−1) and (2), (−2) have become prototype systems towards the experimental and theoretical attempts to the atom–triatom (diatom–diatom) reactive scattering problem.

Experimental investigations of reaction (1) and its isotopically substituted counterparts, in which the effect of reagent translational and/or vibrational excitation on the dynamics was studied, were reported by several working groups [2–4]. In ref. [5], the rotational and vibrational excitation of water molecules by translationally excited H atoms was investigated. Recently, first reaction dynamics studies of reaction (−1) were also carried out [6], [7] [#1].

Following the classic experiments of Oldershaw and Porter [8] on reaction (2), a variety of gas-phase reaction dynamics experiments employing the "hot" H atom technique were performed [9–11]. Inelastic collisions of "hot" H atom with CO_2 were investigated in detail by Flynn and Weston and their results reviewed in ref. [12]. Reaction dynamics investigations of reaction (−2) were carried out using vibrationally excited CO molecules [13] as well as translationally excited OH radicals [14]. Further reaction

[#1] Special issue in honour of John C. Polanyi on the occasion of his 65th birthday.

0009-2614/94/$07.00
SSDI 0009-2614(93)E1462-P

dynamics studies focused on the vibrational-state distribution [15] and the angular and velocity distribution of CO_2 produced in reaction (−2) [16] as well as on inelastic collisions between OH and CO [17].

In addition, experiments were carried out using CO_2...HX van der Waals (vdW) complexes (X = HS, Cl, Br, I) to study the influence of reactant orientation on the reactivity [18] and the OH product state distributions [19,20] of reaction (2). The first real-time measurements of product formation from a bimolecular reaction were carried out by Zewail and co-workers [21]. In these pioneering experiments, reaction (2) was photo-initiated in CO_2...HI vdW complexes using a picosecond photodissociation pulse and the OH radicals produced were detected in real-time by a subsequent picosecond probe pulse. Recently, Wittig and co-workers have carried out similar measurements with sub-picosecond time resolution [22]. Within the uncertainty limits of the I–HOCO translational recoil energies, good agreement between their experimental reaction rates and the results of quasiclassical trajectory (QCT) calculations [23] as well as with the results from recent quantum-scattering (QMS) calculations [24] was found.

On the other hand, the so-called "velocity-aligned photofragment dynamics technique" pioneered by Hancock and co-workers, and Simons and co-workers, which has already been successfully used to examine stereochemical attributes of a variety of bimolecular reactions [25–32], has not yet been applied to reactions (1) and (2).

In the present work we have determined both scalar properties like OH rotational and vibrational energy/quantum state distributions as well as vector properties, in particular OH product angular momentum centre-of-mass alignment parameters $A_0^{(2)}$ (c.m.) for reaction (1) and (2) at different collision energies.

2. Experimental technique

The experiments were carried out using the laser photolysis/laser-induced fluorescence (LP/LIF) "pump–probe" technique. It is essentially the same method already used to measure OH product quantum state distributions for reactions like e.g. $H+O_2$ [33]. The experimental apparatus is depicted schematically in Fig. 1. The experiments were carried out in flowing mixtures of H_2S (UCAR, electronic grade) and room temperature H_2O (doubly distilled and degased prior to use) and CO_2 (>99.8%, Messer Griesheim), respectively, with a ratio of 1 : 10 at a total pressure of typically 55–70 mTorr (measured by a MKS Baratron).

Translationally excited H atoms having an isotropic velocity distribution were generated by photodissociation of the H_2S precursor using the unpolarized output of an ArF excimer laser (Lambda LPX 205, emission wavelength 193.3 nm). To generate velocity-aligned H atoms, the ArF output was linearly polarized (around 95% polarization) using a 10-plate Brewster-angle stack polarizer (total transmission about 55%). The degree of polarization was checked with a second identical stack polarizer in a polarizer/analyzer arrangement. The same polarizer was used to verify that initially, the 193 nm excimer laser beam was genuinely unpolarized. A circular diaphragm with an aperture of 3 mm was used to skim off a homogenous irradiated part of the unfocused

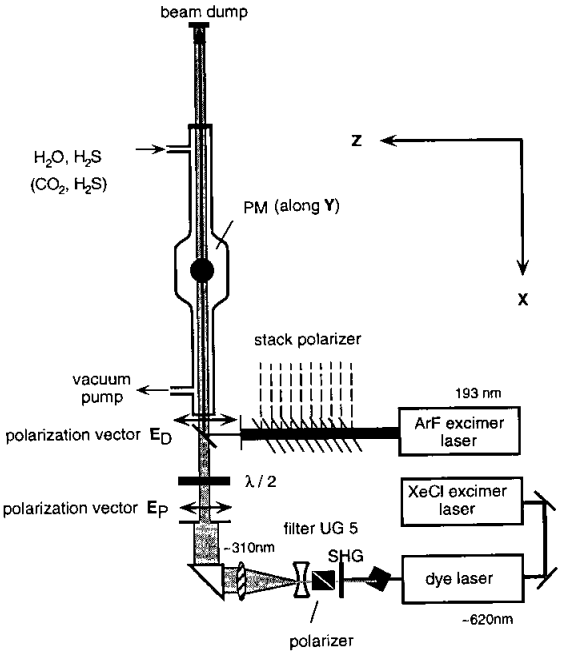

Fig. 1. Schematic diagram of the experimental apparatus for $E_P \| E_D \| Z$. The detector (PM = photomultiplier) is directed along Y (see also Fig. 2).

rectangular excimer profile to provide the photolysis beam. Typical energies of 2 mJ/pulse were used in the experiment. At this energy the OH signals from the reactions showed a linear dependence on the photolysis laser intensity, and no OH background was detectable when only H_2O was present. With these pulse energies the H atom contribution from secondary dissociation of HS is less than 1% [34].

Typically 60–150 ns after the photodissociation ("pump"), the nascent OH product radicals were probed by a second copropagating ("probe") laser beam by laser-induced fluorescence in the $A\,^2\Sigma^+ \leftarrow X\,^2\Pi$ system. Both lasers were triggered by a delay generator (SRS 345, with a GPIB interface) and operated at a repetition rate of 20 Hz. The UV probe beam (bandwidth 0.2 cm^{-1}) in the wavelength region of 305–325 nm was provided by a frequency-doubled dye laser (Lambda FL/2002/EC), pumped by a XeCl excimer laser (Lambda EMG/201/MSC). Using an intra-cavity etalon, the bandwidth could be reduced to 0.09 cm^{-1}, narrow enough to resolve OH Doppler profiles. For the alignment measurements the UV output was completely linearly polarized (>99%) using a Glan-Taylor polarizer. A $\lambda/2$ plate was used to adjust the probe laser polarization vector E_P to any desired angle (ϑ in Fig. 2) with respect to the fixed direction of the photodissociation laser polarization vector E_D. To ensure a linear dependence of the OH fluorescence on the probe laser intensity, the probe beam was attenuated and expanded to a diameter of 10 mm and aligned to overlap the 3 mm diameter photolysis beam. OH fluorescence was collected by a lens and projected upon the cathode of a photomultiplier (EMI 9781 B) mounted perpendicular to the laser beams' axis. The LIF signal as well as photolysis and probe laser intensities (measured with photodiodes) were recorded with a 3-channel boxcar system (SRS 250) and transferred to a microcomputer (HP 9000/320) via an analog-to-digital converter (SRS 235). OH fluorescence signals were normalized to both laser intensities. In the alignment experiments base line checks were carried out for the different polarization configurations, to account for the polarization dependence of the signal background.

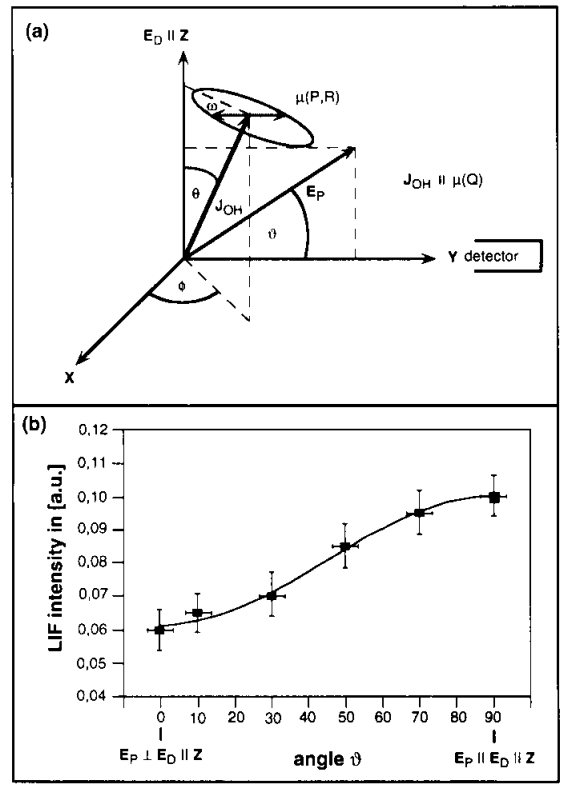

Fig. 2. (a) Scheme of the polarization geometry. *X*, *Y* and *Z* denote the laboratory-frame coordinate axis. The laser beams copropagate along *X*. (b) Relative LIF intensity of $Q_1(9)$ line from reaction (1) as a function of the angle ϑ between E_P and E_D.

3. Experimental results

3.1. OH product scalar properties

Relative number densities of OH fine-structure states were calculated from digitized LIF spectra (recorded between 306.5 and 325 nm, where most of the OH(0–0, 1–1) transitions are located [35]) by numerical integration (taking into account the different Einstein coefficient of absorption [36]).

In Figs. 3 and 4 relative populations of the OH(v=0) rotational fine-structure states from reaction (1) and reaction (2), respectively, are plotted against the rotational quantum number K (as defined in Hund's case b). From the fine-structure distributions we determined the average OH(v=0) rotational energy to be $\langle E_{rot} \rangle = 0.07 \pm 0.02$ eV for reaction (1) and $\langle E_{rot} \rangle = 0.16 \pm 0.02$ eV for reaction

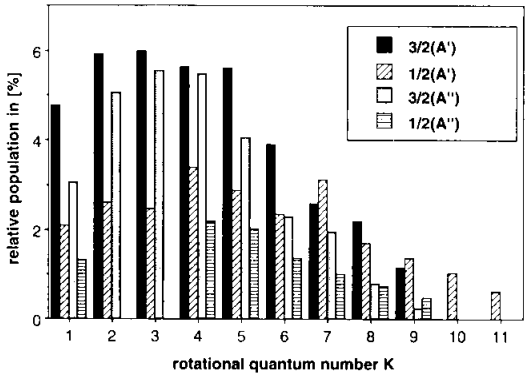

Fig. 3. Population distribution of the OH(v=0) rotational fine-structure states from reaction (1) at $E_{c.m.}$=2.2 eV.

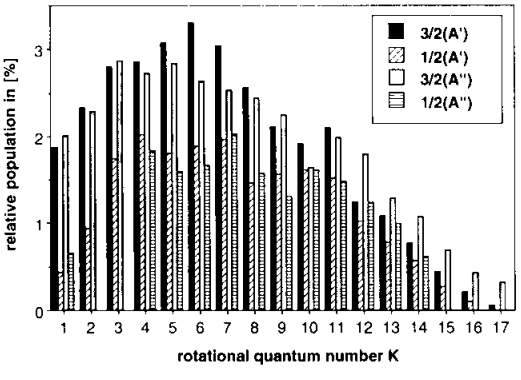

Fig. 4. Population distribution of the OH(v=0) rotational fine-structure states from reaction (2) at $E_{c.m.}$=2.3 eV.

(2). In the case of reaction (1), we could not detect any vibrationally excited OH radicals. From the S/N ratio we determined the upper limit for the OH(v=1)/OH(v=0) ratio to be 0.01. For reaction (2) we measured the OH(v=1)/OH(v=0) ratio to be 0.29±0.09. The OH(v=1) rotational distribution from (2) was found to be similar to that of the vibrational ground state. From the measured OH(v=1)/OH(v=0) ratio the total population of the OH(v=2) state was determined to be 0.03 (using "surprisal" extrapolation [37]). OH translational energies were determined from non-overlapping OH(v=0) Q- and P-branch Doppler line profiles by numerical deconvolution assuming a Gaussian probe laser profile. For reaction (2), Doppler line profiles were also recorded in the OH(1–1) R-branch region. By weighted averaging over the recorded rotational states, following the method described in ref. [10], we calculated the average product center-of-mass translational energy to be $\langle\langle E_{trans}\rangle\rangle$ = 1.02±0.38 eV for (1). For reaction (2), values of $\langle\langle E_{trans}\rangle\rangle^{v=0}$=0.83±0.16 eV and $\langle\langle E_{trans}\rangle\rangle^{v=1}$= 0.37±0.08 eV were determined from OH(v=0) and OH(v=1) Doppler profiles, respectively. Here, double brackets denote that these values represent an average over the probed rotational states as well as over the product laboratory velocity distribution. From the above values we calculated the fraction of the available energy, which appears as relative produce translational energy (f_{trans}), as well as the fraction appearing in the OH rotational (f_{rot}) and vibrational (f_{vib}) degree of freedom, to be f_{trans}=0.65±0.26, f_{rot}=0.04±0.01 and $f_{vib}<4\times10^{-3}$ for reaction (1), and f_{trans}=0.59±0.16 (calculated by weighted averaging $\langle\langle E_{trans}\rangle\rangle^{v=0}$, $\langle\langle E_{trans}\rangle\rangle^{v=1}$ using the measured OH(v=0)/OH(v=1) population ratio), f_{rot}= 0.14±0.02 and f_{vib}=0.11±0.02 for reaction (2).

In the case of reaction (2), experimental data concerning the internal excitation of the CO reaction products was reported at $E_{c.m.}$=2.3 eV, for which the value $f_{CO(rot+vib)}$=0.15, reported by Wittig and coworkers [38], is in excellent agreement with the value, $f_{CO(rot+vib)}$=0.16±0.05, calculated from the present experimental results. Also the slightly higher value, $f_{CO(rot+vib)}$=0.2, reported by Rice and Baronavski [39], is – within the experimental error limit – in agreement with the present results.

For reaction (1), until now, no measurements of the H_2 internal excitation have been carried out at $E_{c.m.}$=2.2 eV. In Zare's group the internal excitation of HD from H+D_2O was studied and a value of $f_{HD(rot+vib)}$=0.47 was determined at $E_{c.m.}$=2.7 eV [40].

In Fig. 5a, the population ration $\Pi(A')/\Pi(A'')$ in the $\Pi_{3/2}$ manifold (for which most rotational levels populated in the reaction can be probed by non-overlapping R- and Q-line transitions) obtained in reaction (1) is plotted. In addition, the population ratio of the spin–orbit components $\Pi_{3/2}/\Pi_{1/2}$ (weighted by $K/(K+1)$ to account for the different degeneracies) is also included. $\Pi(A')/\Pi(A'')$ and $\Pi_{3/2}/\Pi_{1/2}$ ratios for reaction (2) are depicted in Fig. 5b. For both reactions we found a comparable slight preferential population of the low-energy $\Pi_{3/2}$ spin–orbit component, with some weak dependence on the rotational state being probed. By averaging over all ro-

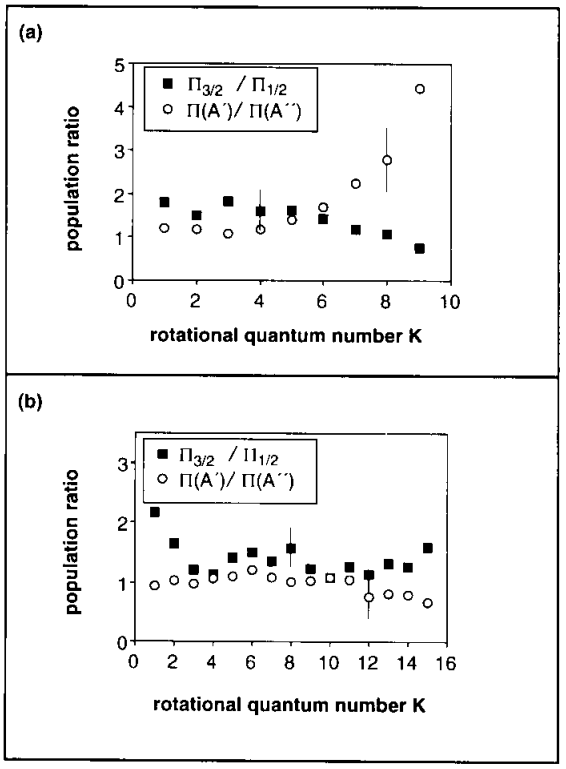

Fig. 5. (a) Population ratio $\Pi(A')/\Pi(A'')$ of the OH($v=0$) Λ-components and the spin–orbit components $\Pi_{3/2}/\Pi_{1/2}$ for reaction (1). (b) Population ratio $\Pi(A')/\Pi(A'')$ of the OH($v=0$) Λ-components and the spin–orbit components $\Pi_{3/2}/\Pi_{1/2}$ for reaction (2).

tational states populated in the reactions we determined the $\Pi_{3/2}/\Pi_{1/2}$ spin–orbit population ratio to be $\langle\Pi_{3/2}/\Pi_{1/2}\rangle = 1.48 \pm 0.25$ for reaction (1), and $\langle\Pi_{3/2}/\Pi_{1/2}\rangle = 1.39 \pm 0.27$ for reaction (2), respectively. Similar behaviour was found in previous studies of (1) and (2) at different collision energies. In ref. [41], Zare and co-workers reported values for $\langle\Pi_{3/2}/\Pi_{1/2}\rangle$ between 1.11 and 1.54 for OH/OD ($v=0$) radicals produced in the reactions H + HOD/D_2O/H_2O. An average spin–orbit population ratio of 1.28 ± 0.14 was reported in ref. [11] (for $K > 3$) for (2), at a collision energy of 1.9 eV.

On the other hand, the relative population of the OH Λ-components $\Pi(A')$ and $\Pi(A'')$ is markedly different for reaction (1) and (2). The $\Pi(A')/\Pi(A'')$ ratio for reaction (1) increases from approximately unity at low K to a value of about 3 at the highest rotational states probed. Similar behaviour of the OH/OD $\Pi(A')/\Pi(A'')$ ratio, namely an increasing ratio with increasing K – as OH/OD coupling cases change from Hund's case (a) to (b) – have been found in several studies of reaction (1) and its deuterated counterparts [2,3,7] as well as in inelastic scattering experiments of OH($^2\Pi_{3/2}$) with H_2 [42].

By way of contrast, the $\Pi(A')/\Pi(A'')$ ratio for reaction (2) is almost constant over the range of rotational states populated in the reaction, with an average value of $\langle\Pi(A')/\Pi(A'')\rangle = 0.97 \pm 0.15$. A comparable value of $\langle\Pi(A')/\Pi(A'')\rangle = 0.98 \pm 0.17$ was reported in the above-mentioned study of reaction (2) at 1.9 eV [11]. Similar values were also obtained at 2.6 eV in Wittig's group [19]. A Λ-ratio of unity was found by Liu and co-workers in inelastic scattering experiments of OH($^2\Pi$) with CO [17].

3.2. OH product vector properties

In the OH product rotational alignment studies, velocity-aligned translationally excited H atoms were generated by linearly polarized 193 nm photodissociation of H_2S, which has been studied in detail by several groups [43,44]. In a recent study in Lee's group, the value -0.94 for the H fragment anisotropy parameter (β_H) in the 193 nm photodissociation of H_2S was confirmed [34], which clearly shows that the primary excitation step of H_2S (at 193 nm) is an almost perpendicular transition followed by a subsequent rapid dissociation with the H atom flight direction being preferentially $\sin^2$-aligned along $\boldsymbol{E}_D$ (i.e. $\boldsymbol{k} \perp \boldsymbol{E}_D$, where $\boldsymbol{k}$ is a unit vector in the H fragment recoil direction).

OH radicals produced in the reaction of velocity-aligned H atoms with H_2O and CO_2 were detected by LIF using a linearly polarized analysis laser. The relative population of different rotational levels (in the high J limit) was measured as a function of the angle ϑ (see e.g. fig. 2a) between the direction of the dissociation polarization vector $\boldsymbol{E}_D$ and the probe laser polarization vector $\boldsymbol{E}_P$ using OH-Q_1-branch transitions. Q-lines were used, because in this case in the limit of high J, the transition moment $\boldsymbol{\mu}(Q)$ lies along $\boldsymbol{J}_{OH}$ (for P- and R-lines it rotates in the plane of rotation, as schematically depicted in Fig. 2a) [45]. Thus, because the excitation probability is given by $|\boldsymbol{\mu}(Q) \cdot \boldsymbol{E}_P|^2$, for Q-lines larger polarization effects are expected.

In both reactions we found a higher population of the rotational states being probed for $\boldsymbol{J}_{OH} \| \boldsymbol{E}_D \perp \boldsymbol{k}$. In Fig. 2b, the variation of the relative OH-Q_1 (9) LIF intensity $I(\vartheta)$ is plotted as a function of the angle ϑ between $\boldsymbol{E}_P$ and $\boldsymbol{E}_D$ for reaction (1). Several measurements were carried out for $J_{OH}=8.5, 9.5$ in case of reaction (1) and for $J_{OH}=9.5, 10.5, 14.5$ in case of reaction (2). Values for $I(\vartheta=90°)=I(\boldsymbol{E}_P \| \boldsymbol{E}_D \| \boldsymbol{Z})$ and $I(\vartheta=0°)=I(\boldsymbol{E}_P \perp \boldsymbol{E}_D \| \boldsymbol{Z})$ were determined by fitting the measured data points (as depicted in Fig. 2b) using a function of the form $F(\vartheta)=a_1+a_2\sin^2(\vartheta)$, where a_1, a_2 are fit parameters, taking $I(90°)=F(90°)$ and $I(0°)=F(0°)$. Our experimental excitation/detection geometry, as depicted schematically in Figs. 1 and 2a, is essentially the same as used by Andresen and co-workers in their H_2O photodissociation dynamics studies [46].

In general, the laboratory-frame distribution of the OH product angular momentum vectors, $\boldsymbol{J}_{OH}$, with respect to the fixed direction defined by $\boldsymbol{E}_D$ can be described by

$$w(\boldsymbol{J}_{OH}, \boldsymbol{E}_D)=[1+\alpha P_2(\boldsymbol{J}_{OH}\cdot\boldsymbol{E}_D)]/4\pi\,. \tag{4}$$

P_2 is the second Legendre polynomial and α is the quadrupole moment, which can be determined from the measured intensity ratio $R=I(90°)/I(0°)$, using the following equation:

$$R=\frac{c_J^2(7+\frac{41}{14}\alpha)+d_J^2(6.5-\frac{17}{14}\alpha)}{c_J^2(6-\frac{15}{14}\alpha)+d_J^2(7+\frac{11}{7}\alpha)}\,. \tag{5}$$

The coefficients c_J^2, d_J^2, defined in ref. [46], describe the J-dependent Λ-doublet mixing in the OH radical and account for the fact that for Q-line excitation $\boldsymbol{\mu}(Q)$ is strictly parallel to $\boldsymbol{J}$ only in the high-J limit. Due to the small effect of the proton hyperfine structure (hfs) on the measured intensity ratio for the J values probed (for a detailed discussion see ref. [46]) no hfs corrections have been included in Eq. (5).

Following ref. [47], we determined the centre-of-mass frame alignment parameter $A_0^{(2)}$(c.m.) defined by

$$A_0^{(2)}(\text{c.m.}):=2\langle P_2(\boldsymbol{J}_{OH}\cdot\boldsymbol{k})\rangle \tag{6}$$

(here and in the following brackets $\langle\ \rangle$ imply an expectation value averaged over all angles), where $\boldsymbol{k}$ is the H atom fragment recoil velocity, using the azimuthally averaged addition theorem [48]

$$\langle P_2(\boldsymbol{J}_{OH}\cdot\boldsymbol{E}_D)\rangle=\langle P_2(\boldsymbol{J}_{OH}\cdot\boldsymbol{k})\rangle\langle P_2(\boldsymbol{k}\cdot\boldsymbol{E}_D)\rangle \tag{7}$$

from the laboratory-frame alignment parameter

$$A_0^{(2)}(\text{lab})=2\langle P_2(\boldsymbol{J}_{OH}\cdot\boldsymbol{E}_D)\rangle=\tfrac{2}{5}\alpha\,, \tag{8}$$

to be

$$A_0^{(2)}(\text{c.m.})=2\alpha/\beta^H\,. \tag{9}$$

In Eq. (9), $\beta^H=5\langle P_2(\boldsymbol{k}\cdot\boldsymbol{E}_D)\rangle$ is the H fragment anisotropy parameter [49]. Using Eq. (9), $A_0^{(2)}$(c.m.) values were determined from the measured intensity ratios, R, for reaction (1) and (2) to be $A_0^{(2)}(\text{c.m.})=-0.94$ $(+0.11-0.14)$ and $A_0^{(2)}(\text{c.m.})=0.07$ $(+0.06-0.11)$, respectively. Using the formulas derived in ref. [50] we found that for the present precursor and target mass ratios and the present average relative velocities, reactant alignment degradation due to the isotropic thermal motion of the precursor and target molecule can be neglected.

An angular momentum centre-of-mass frame alignment parameter, as found for reaction (1), corresponds to the limiting case ($A_0^{(2)}(\text{c.m.})=-1$) in which the OH product angular momentum vector, $\boldsymbol{J}_{OH}$, is perpendicular to the relative velocity vector $\boldsymbol{k}$. For reaction (2), the angular momentum centre-of-mass frame alignment is substantially lower. Thus, in reaction (2) the distribution of $\boldsymbol{J}_{OH}$ with respect to $\boldsymbol{k}$ is more isotropic (for a completely isotropic distribution $A_0^{(2)}$(c.m.) equals zero, in the limiting case where $\boldsymbol{J}_{OH}$ is parallel to $\boldsymbol{k}$, $A_0^{(2)}$(c.m.) equals 2). This is consistent with the interpretation that reaction (2) proceeds via a complex mechanism with a lifetime comparable to the rotational period of the $HOCO^+$ intermediate, while reaction (1) proceeds via a direct mechanism with the H–HOH lifetime being considerably smaller than a rotational period.

4. Discussion

For both reactions we found that product energy distribution is markedly biased, favouring product translational excitation.

The low OH rotational excitation and the absence of OH product vibration in reaction (1) is generally in good agreement with results of QCT [51] and recent QMS calculations [52] on an ab initio PES. In

the case of reaction (1), the non-statistical energy partitioning as well as the observed strong angular momentum alignment can be explained by a direct abstraction mechanism in which the OH bond plays the role of a spectator during the reactive collision.

In the case of reaction (2), a measured $OH(v=1)/OH(v=0)$ population ratio, close to the statistical "prior" value, and the small $A_0^{(2)}$(c.m.) value suggests that at $E_{c.m.}=2.3$ eV, reaction (2) takes place on a time scale for which the $HOCO^+$ rotational period sets an upper limit of about 1.2 ps [53]. This would allow $HOCO^+$ to vibrate about 15 periods in the lowest frequency mode, long enough to ensure complete intramolecular vibrational redistribution (IVR). At a nominal gas-phase $E_{c.m.}$ of about 2.1 eV, a $HOCO^*$ lifetime of 1 ps has been determined in a real-time study (with picosecond resolution) of reaction (2) (photo-initiated in CO_2...HI vdW complexes) [21]. On the other hand, OH product buildup times of about 250 fs have been measured [22] (with sub-picosecond resolution) in the same environment and at comparable collision energies which, despite the fact that such small buildup times raise the question whether in about three $HOCO^+$ vibrational periods complete IVR is still possible, are in surprisingly good agreement with earlier RRKM predictions [10]. In QCT calculations on ab initio PES (constructed to describe the gas-phase reactions (2) and (−2)), a $HOCO^*$ lifetime of 0.4 ps was found at a comparable total energy [54]. However, QCT calculations on the same PES for $E_{c.m.}=2.3$ eV lead to about a factor of 1.7 higher CO internal excitation and to about a factor of 1.5 higher OH rotational excitation than found in the experiment of Rice and Baronavski [39], and in our present one, respectively. This suggests that corrections of the PES, at least in the HO–CO saddle point region, are necessary. In addition, for a detailed understanding of the variety of reaction pathways and mechanisms which are possible when reaction (2) is photo-initiated in CO_2...HI vdW complexes, the development of full CO_2...HI ab initio ground state and excited state PESs and subsequent dynamical studies of the photo-initiated reactive processes are clearly needed.

5. Acknowledgement

The financial support of the Deutsche Forschungsgemeinschaft is gratefully acknowledged. The authors wish to thank D. David, T. Dreier and A. Suvernev for helpful discussions and M. Brouard, J. Rice, G.C. Schatz, and C. Wittig for sending preprints of their publications. Thanks are also due to P. Monkhouse for many helpful comments during the preparation of the manuscript.

6. References

[1] W.M. Smith and R. Zellner, J. Chem. Soc. Faraday Trans. II 69 (1973) 1617;
J. Warnatz, Ber. Bunsenges. Physik. Chem. 87 (1983) 1008;
J. Wolfrum, in: 20th International Symposium on Combustion (The Combustion Institute, Pittsburgh, 1984) p. 559;
J. Troe, in: 22nd International Symposium on Combustion (The Combustion Institute, Pittsburgh, 1988) p. 843.

[2] K. Kleinermanns and J. Wolfrum, Appl. Phys. B 34 (1984) 5;
K. Honda, M. Takayanagi, T. Nishiya, H. Ohoyama and I. Hanazaki, Chem. Phys. Letters 180 (1991) 321;
A. Jacobs, H.-R. Volpp and J. Wolfrum, in: 24th International Symposium on Combustion (The Combustion Institute, Pittsburgh, 1992) p. 605; Chem. Phys. Letters 196 (1992) 249;
K. Kessler and K. Kleinermanns, Chem. Phys. Letters 190 (1992) 145;
A. Jacobs, H.-R. Volpp and J. Wolfrum, J. Chem. Phys., in press.

[3] M.J. Bronikowski, W.R. Simpson, B. Girad and R.N. Zare, J. Chem. Phys. 95 (1991) 8647;
M.J. Bronikowski, W.R. Simpson and R.N. Zare, J. Phys. Chem. 97 (1993) 2204.

[4] A. Sinha, M.C. Hsiao and F.F. Crim. J. Chem. Phys. 92 (1990) 6333;
A. Sinha, J. Phys. Chem. 94 (1990) 4391;
F.F. Crim, M.C. Hsiao, J.L. Scott, A. Sinha and R.L. van der Wal, Phil. Trans. Roy. Soc. Ser. A 332 (1990) 259;
A. Sinha, M.C. Hsiao and F.F. Crim, J. Chem. Phys. 94 (1991) 4928;
M.C. Hsiao, A. Sinha and F.F. Crim, J. Phys. Chem. 95 (1991) 8263;
F.F. Crim, S. Sinha, M.C. Hsiao and J.D. Thoemke, in: Mode selective chemistry, eds. J. Jortner, R.D. Levine and B. Pullman (Kluwer, Dordrecht, 1991) p. 217.

[5] C.M. Lovejoy, L. Goldfarb and S.R. Leone, J. Chem. Phys. 96 (1992) 7180.

[6] M. Alagia, N. Balucani, P. Casavecchia, D. Stranges and G.G. Volpi, J. Chem. Phys. 98 (1993) 2459.

[7] S. Koppe, T. Laurent, P.D. Naik, H.-R. Volpp and J. Wolfrum, Can. J. Chem., in press.
[8] G.A. Oldershaw and D.A. Porter, Nature 223 (1969) 490.
[9] R.E. Tomalesky and J.E. Sturm, J. Chem. Soc. Faraday Trans. 68 (1972) 1241;
C.R. Quick and J.J. Tiee, Chem. Phys. Letters 100 (1983) 223;
K. Kleinermanns and J. Wolfrum, Laser Chem. 2 (1983) 339; Chem. Phys. Letters 104 (1984) 157;
K. Kleinermanns, E. Linnebach and J. Wolfrum, J. Phys. Chem. 89 (1985) 2525.
[10] G. Hoffmann, D. Oh, Y. Chen, Y.M. Engel and C. Wittig, Israel J. Chem. 30 (1990) 115.
[11] A. Jacobs, M. Wahl, R. Weller and J. Wolfrum, Chem. Phys. Letters 150 (1989) 161.
[12] G.W. Flynn and R.E. Weston Jr., J. Phys. Chem. 97 (1993) 8116.
[13] T. Dreier and J. Wolfrum, in: 18th International Symposium on Combustion (The Combustion Institute, Pittsburgh, 1981) p. 801.
[14] J. Wolfrum, Faraday Discussions Chem. Soc. 84 (1987) 191; Spectrochim. Acta A 46 (1990) 567.
[15] M.J. Frost, P. Sharkey and I.W.M. Smith, Faraday Discussions Chem. Soc. 91 (1990) 305.
[16] P. Casavecchia, N. Balucani and G.G. Volpi, in: Research in chemical kinetics, eds. R.G. Compton and G. Hancock (Elsevier, Amsterdam, 1993).
[17] D.M. Sonnenfroh, R.G. Macdonald and K. Liu, J. Chem. Phys. 94 (1991) 6508.
[18] S.K. Shin, C. Wittig and W.A. Goddard III, J. Phys. Chem. 95 (1991) 8048.
[19] S. Buelow, G. Radhakrishnan, J. Catanzarite and C. Wittig, J. Chem. Phys. 83 (1985) 444;
S. Buelow, G. Radhakrishnan and C. Wittig, J. Phys. Chem. 91 (1987) 5409.
[20] G. Radhakrishnan, S. Buelow and C. Wittig, J. Chem. Phys. 84 (1986) 727.
[21] N.F. Scherer, L.R. Khundkar, R.B. Bernstein and A.H. Zewail, J. Chem. Phys. 82 (1987) 1451;
A.H. Zewail, Science 242 (1988) 1645;
N.F. Scherer, C. Sipes, R.B. Bernstein and A.H. Zewail, J. Chem. Phys. 92 (1990) 5339.
[22] C. Jaques, L. Valachovic, S. Ionov, E. Böhmer, Y. Wen, J. Segall and C. Wittig, J. Chem. Soc. Faraday Trans. 89 (1993) 1419.
[23] K. Kudla and G.C. Schatz, J. Chem. Phys. 95 (1991) 1635.
[24] D.C. Clary, NATO Adv. Res. Workshop on Orientation and Polarization Effects in Chemical Reaction Dynamics, Perugia, Italy (1992) paper 36.
[25] M. Brouard, S.P. Duxon, P.A. Enriquez and J.P. Simons, J. Chem. Phys. 97 (1992) 7414.
[26] K. Kleinermanns and E. Linnebach, Appl. Phys. B 36 (1985) 203;
J. Wolfrum, J. Phys. Chem. 90 (1986) 375; in: Selectivity in chemical reactions, ed. J.C. Whitehead (Kluwer, Dordrecht, 1988) p. 23;
P.D. Naik, H.-R. Volpp and J. Wolfrum, manuscript in preparation.
[27] G.W. Johnston, S. Satyapal, R. Berson and B. Katz, J. Chem. Phys. 92 (1990) 206.
[28] B. Katz, J. Park, S. Satyapal, S. Tasaki, A. Chattopadhayay, W. Yi and R. Berson, Faraday Discussions Chem. Soc. 91 (1991) 73.
[29] F. Green, G. Hancock and A.J. Orr-Ewing, Faraday Discussions Chem. Soc. 91 (1991) 79.
[30] D.J. Rakestraw, K.G. McKendrick and R.N. Zare, J. Chem. Phys. 87 (1987) 7341.
[31] M. Brouard, S.P. Duxon, P.A. Enriquez, R. Sayos and J.P. Simons, J. Phys. Chem. 95 (1991) 8169; Laser Chem. 11 (1991) 265.
[32] M. Brouard, S.P. Duxon, P.A. Enriquez and J.P. Simons, J. Chem. Soc. Faraday Trans. 89 (1993) 1435.
[33] K. Kleinermanns and J. Wolfrum, J. Chem. Phys. 80 (1984) 181;
K. Kleinermanns, E. Linnebach and M. Pohl, J. Chem. Phys. 91 (1989) 2181;
M.J. Bronikowski, R. Zhang, D.J. Rakestraw and R.N. Zare, Chem. Phys. Letters 156 (1989) 7;
A. Jacobs, H.-R. Volpp and J. Wolfrum. Ber. Bunsenges. Physik. Chem. 94 (1990) 1390; Chem. Phys. Letters 177 (1991) 200.
[34] R.E. Continetti, B.A. Balko and Y.T. Lee, Chem. Phys. Letters 182 (1991) 400.
[35] G.H. Dieke and H.M. Crosswhite, J. Quantum Spectry. Radiative Transfer 2 (1962) 97.
[36] I.L. Chidsey and D.R. Crosley, J. Quantum Spectry. Radiative Transfer 23 (1980) 187.
[37] A. Ben-Shaul, R.D. Levine and R.B. Bernstein, Chem. Phys. Letters 15 (1973) 160;
D. Levine and J.L. Kinsey, in: Atom–molecule collision theory – a guide for the experimentalist, ed. R.B. Bernstein (Plenum Press, New York, 1979) p. 693.
[38] S.L. Nickolaisen, H.E. Cartland and C. Wittig, J. Chem. Phys. 96 (1992) 4378.
[39] J.K. Rice, Y.C. Chung and A.P. Baronavski, Chem. Phys. Letters 167 (1990) 151;
J.K. Rice and A.P. Baronavski, J. Chem. Phys. 94 (1991) 1006.
[40] D.E. Adelman, S.V. Filset and R.N. Zare, J. Chem. Phys. 98 (1993) 4636.
[41] M.J. Bronikowski, W.R. Simpson and R.N. Zare, J. Phys. Chem. 97 (1993) 2194.
[42] P. Andresen, D. Häusler and H.W. Lülf, J. Chem. Phys. 81 (1984) 571;
P. Andresen, N. Aristov, V. Beushausen, D. Häusler and H.W. Lülf, J. Chem. Phys. 95 (1991) 5763.
[43] G.N.A. van Veen, K.A. Mohamed, T. Baller and A.E. de Vries, Chem. Phys. 74 (1983) 261;
X. Xie, L. Schneider, H. Wallmeier, R. Boettner, K.H. Welge and M.N.R. Ashfold, J. Chem. Phys. 92 (1990) 1608.
[44] Z. Xu, B. Koplitz and C. Wittig, J. Chem. Phys. 87 (1987) 1062.

[45] D.A. Case, G.M. McClelland and D.R. Herschbach, Mol. Phys. 35 (1978) 41.
[46] P. Andresen, G.S. Ondrey and B. Titze, J. Chem. Phys. 80 (1984) 2548.
[47] F. Green, G. Hancock, A.J. Orr-Ewing, M. Brouard, S.P. Duxon, P.A. Enriquez, R. Sayos and J.P. Simons, Chem. Phys. Letters 182 (1991) 568.
[48] M.G. Prisant, C.T. Rettner and R.N. Zare, J. Chem. Phys. 75 (1981) 2222.
[49] R.N. Zare, Mol. Photochem. 4 (1972) 1.
[50] E.P. Gilbert, G. Maitland, A. Watson and K.G. McKendrick, J. Chem. Soc. Faraday Trans. 89 (1993) 1527.
[51] G.C. Schatz, J.L. Colton and M.C. Grant, J. Phys. Chem. 88 (1984) 2971;
K. Kudla and G.C. Schatz, J. Chem. Phys. 95 (1991) 8267; Chem. Phys. Letters 193 (1992) 507; J. Chem. Phys. 98 (1993) 4645.
[52] H. Szichman, I. Last, A. Baram and M. Baer, J. Phys. Chem. 97 (1993) 6436;
G. Nyman and D.C. Clary, J. Chem. Phys., accepted for publication.
[53] S. Koppe, P.D. Naik, H.-R. Volpp and J. Wolfrum, manuscript in preparation.
[54] K. Kudla, G.C. Schatz and A.F. Wagner, J. Chem. Phys. 95 (1991) 1635.